UNIVERSITY OF GÄVLE

FACULTY OF ENGINEERING AND SUSTAINABLE DEVELOPMENT
Department of Building Engineering, Energy Systems and Sustainability Science

Integration of a heat recovery system in a Spray Drying Process: Model Simulation Analysis and Economic Feasibility

Marcel Hott Oller

2023

Preface

This thesis has been completed thanks to my father, who has consistently supported me in my studies and career, both financially and as a mentor, imparting valuable engineering practices.

I am also grateful to the company Newcospray S.L.U. for granting me access to their extensive knowledge and data on Spray drying, which has greatly contributed to this study.

Lastly, I express my gratitude to Arman Ameen for his corrections, as well as all the professors I had during my master's degree, whose teachings have greatly enriched the knowledge utilized in this thesis.

Abstract

The spray drying process is widely established in the industry worldwide. However, due to its complexity in predicting variables, the technology is often regarded as a "Black box" process. In this study, a model based on energy and mass balances is designed and validated using Matlab/Simulink software and real data from a medium-sized machinery, specifically the Production Minor manufactured by GEA NIRO S/A. Additionally, the simulation incorporates a heat recovery system based on a heat pump, and its economic feasibility is examined.

The simulation is validated for a narrow range of variables and demonstrates an accuracy of approximately 95% in most cases.

The heat recovery system achieves an average natural gas savings of 0.43 kg/h. However, this saving is accompanied by an additional electrical consumption of 2.1 kW resulting from the operation of the heat pump.

The economic feasibility study of the heat recovery system reveals an extra production cost of 0.1€/h in exchange for a 36% average reduction in natural gas dependency.

Nomenclature

Latin

Symbol	Description	Unit
T	Temperature	ºC
P	Pressure	kPa
M	Moisture	kg water /kg air
$\dot{q}$	Heat transfer	kW
$\dot{W}$	Work	kW
$\dot{m}$	Mass Flow	kg/s
h	Enthalpy	kJ/kg
cp	Specific heat	kJ $ºC^{-1}\ kg^{-1}$
Sld	Solid content in the feed	kg solid/Kg water
s	Entropy	kJ $ºC^{-1}\ kg^{-1}$

Greek

Symbol	Description	Unit
η	Performance	-
Δ	Difference, final minus initial	-

Abbrevations and Acronyms

Symbol	Description
SDP	Spray Drying Process
ATEX	ATmosphere EXplosible
HEPA	High Efficiency Particle Arresting
AF	Air Fuel Value

Table of contents

1 Introduction

1.1 Background

The spray drying process is extensively employed in the food, pharmaceutical, and chemical industries to convert liquids or slurries into dry powders or granules. This method offers precise control over particle size and distribution, leading to consistent and predictable product quality. Due to its widespread usage, numerous studies and investments have been dedicated to improving this process. The research primarily focuses on two areas: enhancing the prediction and control of the obtained product and optimizing the process itself in terms of thermal efficiency and cost-effectiveness. This study aims to provide a detailed explanation of the Spray Drying Process to enhance understanding of the topic.

Despite the widespread implementation of the Spray Drying Process (SDP) across various industries, it remains a black box process, lacking complete understanding of its internal workings. This poses challenges for implementing simulations or physical models and obtaining accurate results. Consequently, empirical models based on real-world data are widely used in industrial settings.

Presently, there exists a notable disparity between the technological landscape observed in the industrial sector and the state-of-the-art underlying processes. Although considerable efforts have been made to enhance the technology's performance, skepticism often arises when it comes to implementing these improvements. This hesitance stems from the black box nature of the process and concerns about disrupting a fully functional process by making changes.

Continuing along the line of performance improvement, numerous research papers aim to reduce energy consumption using various technologies, sometimes drawing upon knowledge and experiences from other research fields. Researchers primarily focus on harnessing the energy present in the system's exhaust air through closed-loop systems or heat recovery techniques. Implementing the necessary technologies to facilitate these alternative approaches is crucial. Given that natural gas serves as the primary energy resource for this process, it is essential to acknowledge the adverse impact on its availability and cost caused by recent global events such as the COVID-19 pandemic and the Ukraine-Russian War. Consequently, recent studies aim to mitigate the reliance on natural gas by either reducing its usage or exploring alternative energy sources, including renewable energies.

1.2 Literature Review

To find the literature that helped the realization of this study, the online tool Ulrich web has been used. Besides, the use of the advanced search for peer-reviewed papers and journals provided a trustful source of information. The key words used are Spray Drying Process, thermal performance and silica. By this procedure, we found journals like Drying Technology an International Journal and Dairy Science & Technology Official journal of the Institut National de la Recherche Agronomique (INRA) Formerly 'Le Lait'. The papers exposed below are mostly from these journals.

To address the challenge of reducing reliance on natural gas, it is indeed common to start by improving the efficiency of the process. By doing so, the objective is to minimize energy consumption, which directly translates to lower natural gas usage. However, the concept of process efficiency requires clarification as it is not a straightforward matter.

There are various approaches to defining performance in this context. One way to measure energy efficiency is by comparing the energy utilized for water evaporation in the feed to the overall energy consumption within the system.

$$\eta = \frac{E_{ev}}{E_{in}} \qquad (1)$$

Where:

- E_{ev} is the energy used to evaporate the water in the feed.

- E_{in} is the energy used in the system.

The following way of describing the efficiency is enough accurate only when the moisture and the convective temperature are low, the process is adiabatic and the specific heat capabilities are constant.

$$\eta = \frac{T_1 - T_2}{T_1 - T_0} \qquad (2)$$

Where:

- T_1 is the air that enter in the drying chamber.

- T_2 is the air that leave out of the drying chamber.

- T_0 is the ambient air.

As it can be seen in the equation above (2), get better efficiencies is possible by letting T1 grow and the outlet air close to the saturation (best case). However, the level of saturation is related to the thermodynamic characteristics of the outlet air and the conditions for saturation inside the chamber. Besides, the main limit for T1 is the resistance to thermal degradation of the fed (slurry raw material), so getting this most efficient case is not common. In addition, it is crucial to note that allowing the temperature (T2) to decrease may also result in the chamber walls becoming wet, which can lead to a catastrophic scenario and significantly hamper production capabilities. This phenomenon occurs because the dry powder adheres to the humid areas, forming clusters of sticky powder that impede its descent. As a result, the obstruction impedes the smooth flow of the powder and creating possible bacteria growth.

The performance can also be defined as how the fraction of useful energy is really evaporating the water of the feed inlet [1].

$$\eta = \frac{energy\ required\ for\ evaporation}{(input\ energy - exhaust\ energy)} \tag{3}$$

While Equation (3) provides valuable insights into evaluating the performance of the drying chamber and the energy exchange between the feed and inlet air, it will not be utilized for the purposes of this study. Since the temperature of the inlet and outlet air is linked to the characteristics of the final product, this study will adopt a modified version of Equation (1) that incorporates the paid energy (E_{in}) used throughout the entire process. The term "paid energy" refers to the energy sourced from natural gas or electricity. Furthermore, considering the reasons previously mentioned, electricity is preferred over gas energy.

Now that the different types of efficiency in a drying process have been defined, the study can proceed to explore methods for enhancing this value and reducing natural gas consumption.

One of the most widely discussed technologies for improving the efficiency of spray drying processes is the implementation of a closed-loop system. This technology aims to utilize the still warm outlet air as the inlet air for the process. To achieve this, it is necessary to dehumidify the outlet air and, ideally, use the energy released during dehumidification to preheat the inlet air. Numerous different approaches exist for energy recovery and dehumidification, each offering varying levels of efficiency and flexibility. The selection of a particular method involves striking a balance between different factors.

Implementing a closed-loop system in the process can result in total savings ranging from 11% to 42%, depending on the specific technique employed.

To obtain these results, a combination of real-world testing and simulations using pinch technology in a computational model has been carried out. These studies explore different configurations of heat recovery systems. Among the various configurations tested, the most efficient one utilizes a membrane contactor with superheated steam. This hydrophobic membrane selectively allows only air to pass through, separating the warm dry air and vapor from the exhaust air stream coming from the drying chamber.

However, a primary challenge associated with this configuration is the potential saturation of the membrane caused by fine particles that are not effectively removed from the exhaust air. Certain studies have observed this issue, leading to the impracticality of applying this technology to products that generate a significant amount of fine particles during the drying process[2].

In current industrial practices, closed-loop systems are typically implemented when the solvent used in the feed is too expensive to be discharged with the exhaust air. This situation arises when the solvent cannot be water. Another scenario where closed loops are utilized is when nitrogen is used as the inlet gas, usually due to the high reactivity of the feed with oxygen. While the technology and experience gained from these processes can be valuable, it is important to note that it may not always be feasible or desirable to implement closed loops in every situation, as discussed in recent papers.

An alternative approach to improving drying efficiency involves increasing the percentage of dry material in the feed. This naturally leads to a higher powder yield while reducing the requirement for water evaporation, thereby enhancing overall process performance. Traditional methods employed for this preliminary process have relied on evaporators, gas-combustion boilers for thermal energy, pressure filters, and decanters. However, a newer technology that has gained attention among researchers is mechanical dewatering. This innovative approach eliminates the need for thermal energy and reduces reliance on natural gas consumption. The research conducted for this study involved searching for new technologies in various journals [3].

In the context of this study and the defined performance criteria, improvements in the feed such as increasing the percentage of dry material are not considered since the energy required for water evaporation remains the same. However, it is worth noting that evaporators typically have better thermal efficiencies compared to spray drying processes.

In line with the global focus on green energy and zero emissions, researchers are actively exploring alternatives to using natural gas for heating the inlet air. Certain products, such as milk powder, require lower inlet temperatures for the drying process. In such cases, the combination of parabolic trough collectors for heating the inlet air and a closed-loop system enables the reduction or elimination of natural gas dependence. Furthermore, the electricity demand for fans and pumps required in the process can be met by connecting them to PV panels, allowing the entire spray drying system to be powered by solar energy [4]. Although the spray drying process improved the efficiency by 53.47% and the exergy efficiency by 11.45%, the overall efficiency of the process is not increased that much because the main part of the drying process has been done by the evaporator which dry more than the 50% of the water content of the initial product (skimmed milk). After all, the vacuum evaporator has a higher drying efficiency. Another innovative technology utilized in this research involves the implementation of a heat pump during the moisture separation stage. This enables the process to recycle energy during condensation, utilizing it to preheat the air before it undergoes heating in the solar collectors. By employing this approach, the system maximizes energy efficiency by effectively utilizing the recovered heat and minimizing energy losses. This research has been done for a production of 1.85 Kg/h of milk powder and a 20m² of solar collectors during the summer season, which is a very little production for milk powder where normally thousands of kilograms are made every hour. This model could be scalable up to industrial size but no comments related with this topic are made. The method used in this paper is computational simulation made with mathematical models which tries to be as realistic as possible [5].
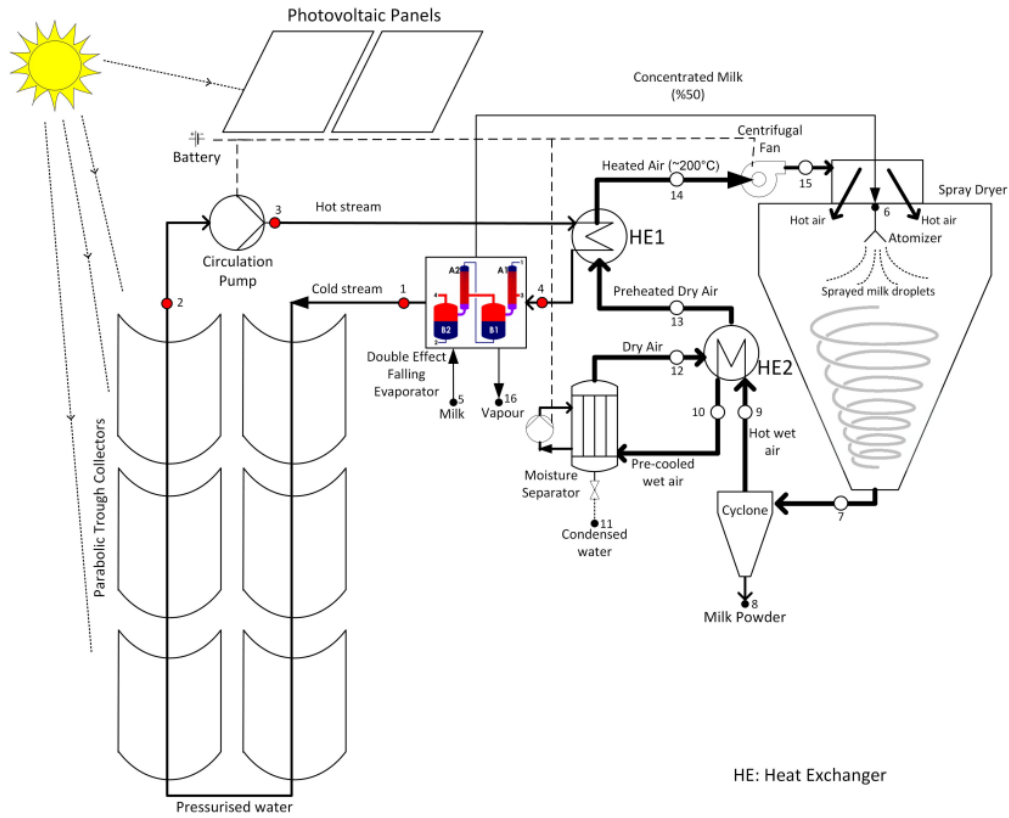
Figure 1: Schematic of the integrated PTC-SP milk powder production system [5].

As depicted in Fig. 1, the closed-loop system reuses the air extracted from the chamber. This proposed solution offers substantial energy-saving potential. However, there is a need for further investigation to assess the potential impact of air reuse on products that are susceptible to bacterial contamination. It is important to evaluate the implications on product safety and establish appropriate measures to mitigate the risk of bacterial infections.

The study relies on mathematical models to understand the behavior of the drying process. It should be noted that numerous sources acknowledge the intricate interactions within the drying chamber, leading to the utilization of "black box" models. These models, which employ predefined input parameters and observe output parameters, aim to realistically capture the relationships between them. Considerable research has been conducted to enhance the accuracy of these models by incorporating mass balance and energy balance equations. While these models perform well in predicting temperatures and moisture percentages of the final powdered product, other parameters such as porosity and grain size are more challenging to precisely predict. [6]

As mentioned earlier, the temperatures of the inlet and outlet air have a direct impact on the desired characteristics of the powdered product. However, it is often challenging to achieve the ideal thermodynamic temperatures in the process due to various reasons. Experimental studies conducted using an SDP plant and concentrated milk have confirmed a close relationship between the outlet temperature and the final moisture content of the powder.

Nevertheless, it is important to acknowledge that the moisture content of the powder is influenced by factors beyond just the temperatures of the inlet and outlet air. Recent experiments have revealed that the absolute water content of the inlet, the mass flow rate of the concentrate, and the temperature of the inlet air also play a significant role in determining the final moisture content of the product. In order to investigate and establish this information, experiments were designed to maintain a constant outlet air temperature while manipulating the other parameters. This experimental approach enabled the researchers to observe varying moisture contents in the milk powder samples, thereby facilitating the identification of these additional influential factors [7].

This valuable information will assist the study in defining the temperature limits within the simulation, taking into account the strict regulations governing these limits. Furthermore, further investigations have revealed the significance of the inlet mass flow rate of air in shaping the final characteristics of the product. The research has demonstrated that a higher inlet mass flow rate results in a shorter residence time and imparts greater kinetic energy to the droplets upon entry into the chamber. To support these findings, the authors conducted experiments in an operational Spray Drying Plant (SDP), utilizing elevated temperatures and varying parameters. [8].

The investigation of closed-loop systems in spray drying is not only motivated by energy efficiency but also by the necessity to comply with strict environmental regulations regarding particle emissions. In this context, the concept of a fully contained system becomes significant. Closed-loop spray drying plants recycle the exhaust air, eliminating the requirement for additional cleaning equipment like bag filters. This approach not only contributes to energy savings but also ensures compliance with environmental standards by minimizing particle emissions [9].

Energy savings in the spray drying process extend beyond the operational phase and encompass the preheating period as well. During the warm-up phase, the system gradually increases the temperatures to reach the desired operating conditions. This gradual temperature rise allows for energy conservation and optimization throughout the entire duration of the process. It is important to note that during this warm-up period, the feed consists only of water instead of concentrate, resulting in a non-production period with ongoing gas consumption. Although this phase is unavoidable at present, it is crucial to acknowledge its existence and consider it while striving to improve the overall performance of the spray drying process, given its significant energy consumption on a global scale. [10]

Since one of the aims of this study is to make a working simulation, the energy balances and mass balances used has been contrasted with same balances in other studies. Besides, the SDP model based in the simulation of the last paper reviewed is very similar to the model simulated in this study. This contrast process has been very useful during the simulation coding. [11]

1.3 Aims

The main objective of this thesis is to develop a simulation model for an open Spray Drying Process (SDP) and validate it using real data from actual machinery. This will involve collecting relevant information about the SDP, such as operating conditions, equipment specifications, and performance parameters. Once the simulation model is established and validated, the focus will shift to incorporating a heat recovery system based on a heat pump. This addition aims to explore the potential energy savings and efficiency improvements that can be achieved through the integration of this new technology. As there is limited real-world information available for this specific configuration, the simulation results will serve as a basis for assessing the feasibility and economic viability of implementing the heat recovery system. The economic feasibility study will involve comparing the energy consumption of the SDP before and after the integration of the heat recovery system. By evaluating the energy savings and the investment required, the study will provide insights into the financial benefits of the heat recovery technology. Overall, the thesis aims to develop a comprehensive understanding of the SDP process through simulation, validate the results using real machinery data, and assess the economic feasibility of implementing a heat recovery system. This research will contribute to the knowledge and practical applications of energy-efficient and cost-effective spray drying processes.

1.4 Approach

The simulation software used is Matlab/Simulink, and the model used is based in the energy balances and mass balances. A simulation for all the sizes of SDP machinery is very difficult to take into reality due the variances of the different characteristics one from another. Because of that, the model is a reflection of the behavior of a single stage plant and medium size. The data used come from a Production Minor by GEA, NIRO S/A.

Furthermore, the developed model is specifically tailored for food production applications, which necessitates the inclusion of a filtering process prior to the drying chamber. Additionally, an indirect gas heater is integrated into the model to provide the necessary heat for the drying process. These components are essential for ensuring the quality and safety of the food product during the drying operation.

2 Theory

The spray drying process is a method used to convert liquids or slurries into dry powders or granules, commonly used in the food, pharmaceutical, and chemical industries. The process involves three main stages: atomization, drying, and powder collection. As we can see in the Fig. 2, in the first stage, the liquid or slurry is inserted into a chamber where it is atomized into small droplets using a high-pressure nozzle or rotary atomizer. These droplets are then mixed with a stream of hot air in the drying chamber, where the hot air rapidly evaporates the liquid from the droplets, leaving behind dry powder or granules. In the final stage, the dry particles are separated from the air using a cyclone separator and/or a bag filter. After this drying process, the outlet air is discharged to the atmosphere.
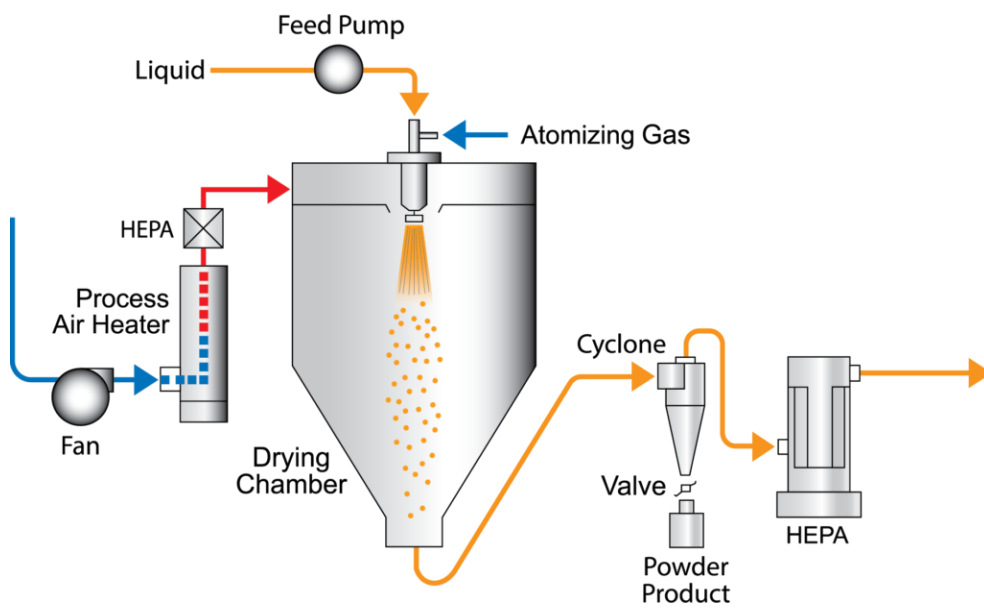

Figure 2: Schematic of an open loop single stage spray drying production system [13].

2.1 Fan

In the plants studied in this thesis, due the relative small dimension of the plant, only one fan is placed at the end of the process line. The fan used is a centrifugal fan that depending on the product should be prepared for ATEX. ATEX (Atmosphères Explosibles) is a regulatory directive in the EU that aims to prevent explosions in areas where flammable substances are present. It sets safety requirements for equipment and provides guidelines for their selection, installation, and maintenance in potentially explosive atmospheres. The fan causes an airflow and a depression in all the ducts of the machinery. The relation of the mass airflow and the pressure is followed the curve shown in the Fig. 3. As the Fig. 3 shows, the selection of a proper fan is determinant because it determinates the mass flow of the entire process. In consequence of this, the evaporation capacity of the SDP is very restricted, only able to vary $\mp 15\%$ of the designed airflow [12].
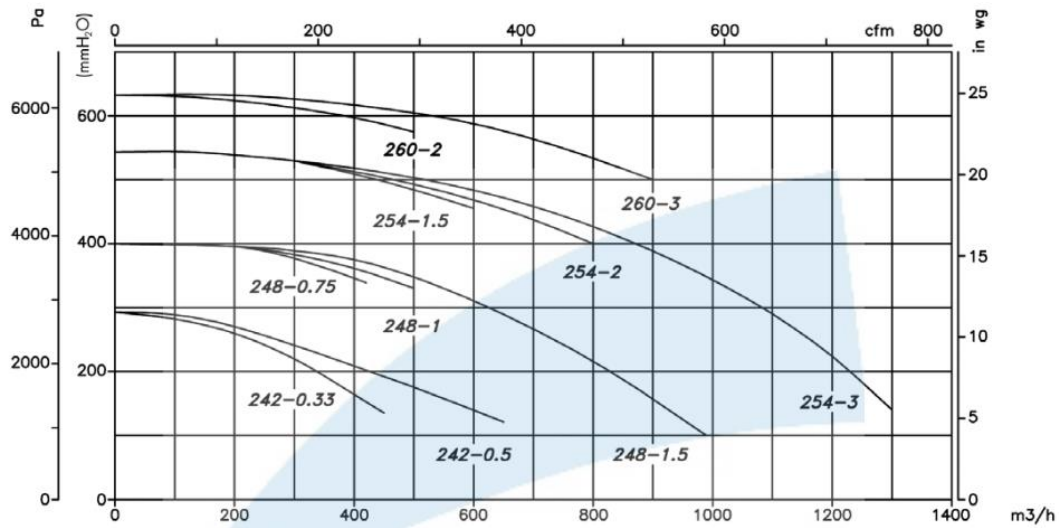

Figure 3: Airflow Pressure curve of different centrifugal fans [14].

2.2 Filter

The filtration of the air process is very closely related with the use of the final powder product. The European normative EN 1822 provides clear guidelines regarding the required level of filtration for various applications. In the case of a process dedicated to food production, such as the one in this study, the minimum filtration requirement specified by EN 1822 is an HEPA (High-Efficiency Particulate Air) filter. This standard ensures that the air quality within the system meets the necessary standards for maintaining a clean and safe environment during food production operations. Because this filter is capable to retain particles of a size until $0.3\ \mu m$ and $1\ \mu m$ pre-filters are needed to avoid the filter clogging in the HEPA. As it can be imaginable, more filter capacity means more drop pressure and energy consumption. Besides, more airflow passing by the filter means even more drop pressure as it can be seen in the Fig. 4. Usually the providers of filters have different size of filter to combine, then the decisions is how many filters the process needs to keep as low as possible the drop pressure.
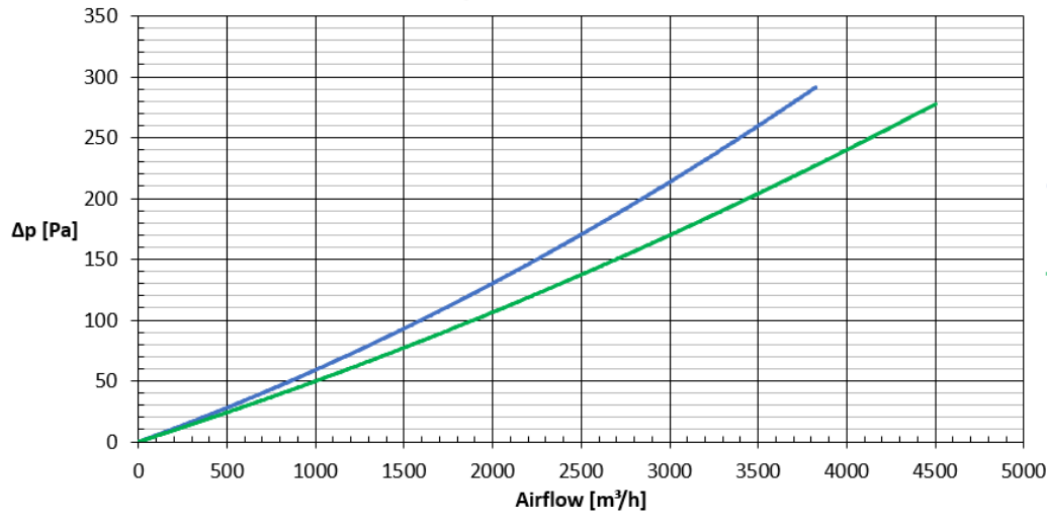

Figure 4: Airflow Pressure curve of different filters [15].

2.3 Heater

The heater is the part of the SDP that consumes more energy. The function of this process unit is to warm the airflow to the inlet airflow temperature of the chamber. This temperature is determined by the process requirements. Airflow heaters can be classified into two main categories: direct and indirect. The main difference between these two types is how they transfer heat to the air.

Direct airflow heaters heat the air by passing it directly over a heat source, such as a heating coil or a burner. The heated air is then blown into the drying chamber. Direct airflow heaters are generally more efficient than indirect airflow heaters since they do not lose heat through a heat exchanger. Although this better performance heating the airflow, the combustion gases are added to the process airflow, providing with them substances like NO_x which are not allowed in high densities in human food products. The electrical direct heaters are clean of particles and pollutant gases but heating the air using just electricity is expensive and not economically viable in relatively big factories. For these reasons, is not possible to use this kind of heater in the model made in this study.

Indirect airflow heaters, on the other hand, heat the air indirectly by passing it over a heat exchanger. In this type of heater, the combustion gases from a burner or other heat source are used to heat a separate chamber containing a heat exchanger. The heat exchanger then heats the air before it is blown into the drying chamber. This heating system is used in process where the inlet air needed must be free of any pollution particle or gas. Because of the way of work, the combustion gases used to warm the inlet air are driven out the system. Due to the widespread usage of this system in food factories, the simulation in this study incorporates the use of an indirect gas heater. However, the source of the warm air is not a crucial factor, making it possible to substitute it with green energy sources such as solar collectors. A more comprehensive theoretical framework is necessary to fully comprehend how the modeling of this system is approached.

The indirect heaters in the industry usually have the natural gas combustion chamber inside the heat exchanger, making this design more efficient since all the heat produced by burner flame is used to warm the process airflow. The temperature of the combustion chamber is determined by the type of gas burned.

The equations used in these heaters are mass balance and energy balance between the two airflows. Following this line, the heat extracted from the combustion gases is the heat received by the process airflow.

$$\dot{Q} = \dot{m} \cdot \Delta h \qquad (4)$$

Where:

- $\dot{Q}$ is the heat transfer.

- $\dot{m}$ is the mass flow.

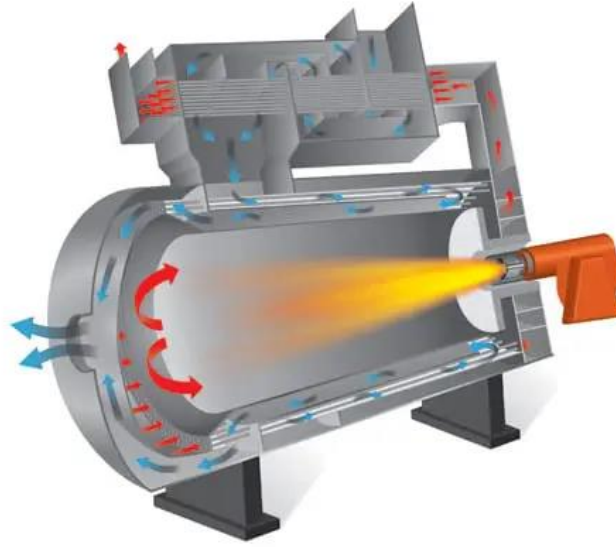- Δh is the difference of the inlet and outlet enthalpies.

Figure 5: Indirect heater schematic [15].

Additionally, considering that the airflow in the system consists of both air and water vapor, the mass flow is divided into two components: the air content and the vapor content. This differentiation becomes even more pronounced in the case of combustion gases, which contain a higher proportion of water vapor due to the combustion reaction. This distinction is crucial since the specific heat of air differs from that of vapor, and accurately accounting for these differences is essential for precise modeling and analysis.

$$\dot{m}_{in} = \dot{m}_{in\,w} + \dot{m}_{in\,a} = \dot{m}_{in} \cdot M_{in} + \dot{m}_{in} \cdot (1 - M_{in}) \qquad (5)$$

Where:

- $\dot{m}_{in}$ is the process air mass flow.

- $\dot{m}_{in\,w}$ is the mass water flow.

- $\dot{m}_{in\,a}$ is the mass air flow.

- M_{in} is the moisture content in the process air mass flow.

To do the energy balance, the mass flow of the combustion gases is needed. To obtain this the natural gas mass flow and the air needed to do the combustion have been considered.

$$\dot{m}_{cg} = \dot{m}_a + \dot{m}_{gas} \qquad (6)$$

Where:

- $\dot{m}_{cg}$ is the mass flow of the combustion gasses.

- $\dot{m}_a$ is the mass air flow coming from the environment.

- $\dot{m}_{gas}$ is the mass gas natural flow.

Then, taking in count that the mass airflow needed to burn the mass gas flow is 9.52 times more and applying the factor AF, the following equation (7) is deduced. The factor AF is used to reflect if the quantity of air is the ideal or more, being the value 1 the ideal mixture.

$$\dot{m}_{cg} = \dot{m}_{gas} \cdot \left(1 + \frac{9,52}{AF}\right) \qquad (7)$$

Where:

- $\dot{m}_{cg}$ is the mass flow of the combustion gasses.

- $\dot{m}_{gas}$ is the mass gas natural flow.

- AF is the Air Fuel ratio.

By this equation, the study assumes that the natural gas is only composed by methane, which is the main component of the gas.

2.4 Drying Chamber

The drying chamber is a critical component of the spray drying process with the temperature, humidity, and airflow controlled. The function of the drying chamber is to provide a controlled environment where the liquid droplets produced by the atomizer can be transformed into dry particles through the process of evaporation. In the spray drying process, the liquid solution or suspension is atomized into small droplets using a high-pressure nozzle or a rotary device. As the droplets leave the atomizer device they are exposed to a stream of warm air, which rapidly evaporates the liquid component of the droplets. The drying chamber is designed to provide a long residence time for the droplets, allowing them to fully evaporate and transform into dry particles. The residence time can be controlled by adjusting the airflow in the drying chamber, as well as the size and shape of the chamber itself. The atomized jet direction also is determinant to the residence time, because of this the drying chambers are divided by this parameter. The name of this division is given following the relative direction versus the inlet air.
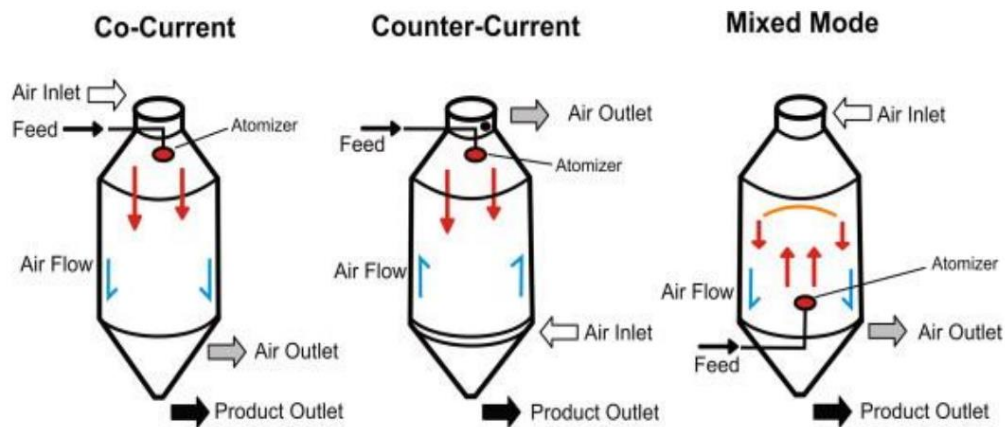

Figure 6: Different types of spray drying chambers [12].

As it has been said, there are different ways to atomize: Rotary devices and nozzle devices. The main difference between the two is the mechanism used to produce droplets. Rotary devices, also known as rotary atomizers, use centrifugal force to produce droplets. In a rotary atomizer, a high-speed spinning disc or wheel is used to atomize the liquid feedstock into droplets. As the liquid is delivered into the spinning disc, it is flung outward by centrifugal force, forming a fine mist of droplets. The nozzle devices, also known as pressure atomizers or spray nozzles, use pressure to produce droplets. In a nozzle device, the liquid feed is pumped at high pressure through a small orifice or nozzle. The high-pressure stream of liquid is then atomized into droplets as it exits the nozzle, due to the shearing forces generated by the high velocity of the liquid as it flows through the nozzle.

Figure 7: On the left, a nozzle atomizing [17]. On the right, a rotary atomizing [18].

The temperature inside the chamber is considered the same as the outlet air stream due the fast evaporation of the water content of the atomized feed. Besides, the dry part of the drop, which is inside a sphere of water when is atomized, is always at the wet bulb temperature of the chamber air. This means that temperature sensitive products can be dried by using this process without destroying the product characteristics.

After the atomization process, it is assumed that there is efficient energy exchange and perfect mixing within the system. Additionally, any losses associated with the process have been deemed negligible and therefore not taken into significant consideration. This assumption allows for simplified modeling and analysis. Following this, and using mass balances and energy balances the following equations are obtained. [12]

$$\dot{m}_{feed} = \dot{m}_{feed\,sld} + \dot{m}_{feed\,w} \tag{8}$$
$$= \dot{m}_{feed} \cdot Sld + \dot{m}_{feed} \cdot (1 - Sld)$$

Where:

- $\dot{m}_{feed}$ is the mass flow in the feed.

- $\dot{m}_{feed\,sld}$ is the solid mass flow in the feed.

- $\dot{m}_{feed\,w}$ is the water mass flow in the feed.

- Sld is the kg of solid per kg of water in the feed.

$$\dot{m}_{in\,w} + \dot{m}_{feed\,w} = \dot{m}_{out\,w} + \dot{m}_{p\,w} \tag{9}$$

Where:

- $\dot{m}_{in\,w}$ is the water mass flow in the inlet air.

- $\dot{m}_{feed\,w}$ is the water mass flow in the feed.

- $\dot{m}_{out\,w}$ is the water mass flow in the outlet air.

- $\dot{m}_{p\,w}$ is the water mass flow in the powder product.

$$\dot{m}_{in\,a} = \dot{m}_{out\,a} \tag{10}$$

$$\dot{m}_{feed\,sld} = \dot{m}_{powder\,sld} \tag{11}$$

Where:

- $\dot{m}_{in\,a}$ is the pure air mass flow in the inlet air.

- $\dot{m}_{out\,a}$ is the pure air mass flow in the outlet air.

- $\dot{m}_{feed\,sld}$ is the solid mass flow of the feed.

- $\dot{m}_{powder\,sld}$ is the solid mass flow of the powder.

$$\dot{m}_{in} \cdot h_{in} + \dot{m}_{feed} \cdot h_{feed} = \dot{m}_p \cdot h_p + \dot{m}_{out} \cdot h_{out} \tag{12}$$

Where:

- $\dot{m}_{in}$ is the mass flow in the inlet air.

- h_{in} is the enthalpy of the inlet air.

- $\dot{m}_{feed}$ is the mass flow in the feed.

- h_{feed} is the enthalpy of the feed.

- $\dot{m}_p$ is the mass flow of the powder obtained.

- h_p is the enthalpy of the powder.

- $\dot{m}_{out}$ is the mass flow in the outlet air.

- h_{out} is the enthalpy of the outlet air.

The enthalpies can be calculated by different procedures depending in what simplifications are taken. In the chamber case and due the relative low difference between the inlet and the outlet temperature and the equal pressure during the process the difference of enthalpies is calculated by using the equation (13).

$$\Delta h = cp \cdot \Delta T \qquad\qquad (13)$$

Where:

- Δh is difference of enthalpies.

- Cp is the specific heat of each component.

- ΔT is difference of temperatures.

2.5   Cyclone and bag filter

The cyclone and the bag filter are the parts of the process dedicated to separate the outlet air of the chamber and the powder obtained in the drying process. The cyclone separate particles from the inlet air by utilizing centrifugal force. It consists of a cylindrical or conical chamber with a tangential inlet and a central outlet for the air stream. As the air stream enters the cyclone, it is forced to spin around the inside of the chamber due to the tangential inlet. As the air spins around the chamber, it creates a centrifugal force that causes the particles to move towards the wall of the chamber. The heavier particles are more strongly affected by this force and are thrown outwards towards the wall of the chamber. The air with the lighter particles and unseparated particles, continues to spin around the center of the chamber and is eventually expelled through the central outlet. This is the first state where powder product is obtained, at least the heavy and big particles. The particles dragged by the air outlet stream, called fines, are transported to the bag filter. The bag filter, as its name indicates, is a filter made by bags which aim is to increase the filtering area. This last step separate the fines from the air stream creating a clean space after the filter and a dusty space before the filter. This process clog the filter quite fast, because of this reason the bag filter has high pressure air streams in the same directions as the bags. This high pressure stream is released every time the differential pressure between the clean space and the dusty space overcome a threshold, cleaning the bags of dust. [12]

Figure 7: On the left, a cyclone [19]. On the right, an open bag filter [20].

This separation process usually is the last step before the exhaust air but, in this thesis, a recovery heat system using a heat pump is studied.

2.6   Heat Pump

A heat pump is a device that is used to transfer heat from one location to another. It works by using a refrigerant to absorb heat from a low-temperature source and then releasing that heat to a high-temperature sink. Heat pumps can be used for heating, cooling, and dehumidification purposes. The basic components of a heat pump include a compressor, an evaporator, a condenser, and an expansion valve. The refrigerant circulates through these components to transfer heat from one location to another.

In this context, the heat pump absorbs heat from the exhaust air source the evaporator. The refrigerant evaporates, absorbing heat from the air, and is then compressed by the compressor, which increases its temperature and pressure. The high-temperature, high-pressure refrigerant then flows through the condenser, where it releases heat to inlet process air. As the refrigerant releases heat, it condenses back into a liquid and is then passed through the expansion valve, where its pressure is reduced, allowing it to return to the evaporator and repeat the cycle. As it can be seen, the selection of the refrigerant is determined, among other things, using the evaporation and condensing temperatures.

Normal oil exchangers usually do this work in the implemented factories. These devices are placed close to the outlet air of the bag filter, where space for big heat exchangers is not possible. Due this limitation, the heat recovered is low. Besides, as bigger heat exchanger means more drop pressure. Nowadays, the heat recovery in big factories suppose to rise the inlet air from 10ºC to 40ºC. [12]
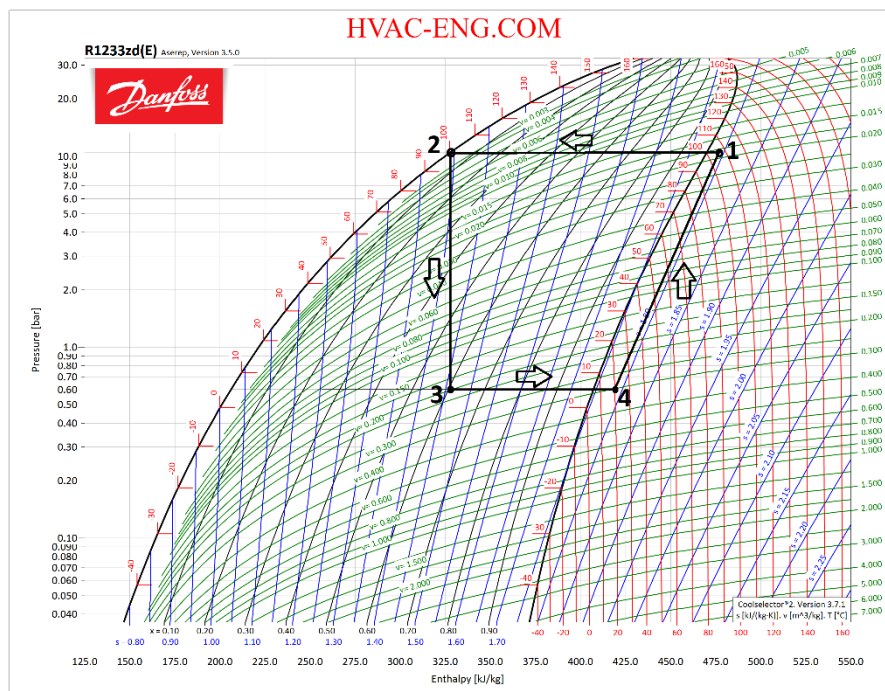

Figure 8: Thermodynamic cycle of a heat pump in a Pressure Enthalpy diagram. [21]

To calculate the energy absorbed from the exhaust air, the energy released to the inlet air and the work done by the compressor, the following equations are used.

$$W_c = h_1 - h_4 \tag{14}$$

$$q_{out} = h_1 - h_2 \tag{15}$$

$$q_{in} = h_4 - h_3 \tag{16}$$

Where:

- W_c work done by the compressor.

- q_{out} heat transfer from the heat pump to the inlet air.

- q_{in} heat transfer from the heat pump to the inlet air.

- h_1, h_2, h_3, h_4 enthalpies in every state of the cycle.

Using a heat pump instead of an air regular exchanger means a much bigger difference of temperatures during both interactions with the air. The point of increase the difference of temperatures is to increase the heat transfer by convection, increasing the pushing force of the transfer.

3 Methods and Process

As the approach chapter explains, the theory has been implemented using the software Matlab/Simulink. This software is very useful for different reasons. First, the way of coding is very visual and clear, helping to visualize the process in a linear way. Second, Being a widely popular software, it has garnered a substantial user base that has developed numerous open-source programs. These user-contributed programs offer valuable functionalities and solutions for diverse situations. Furthermore, the software is well-known and familiar to me, enabling me to provide accurate and relevant information in relation to its capabilities and usage.

To validate the results, utilizing real data is considered the most reliable approach, as demonstrated in this study through the initial open-loop simulation. While it would be beneficial to corroborate the results of implementing the heat pump with real experiments, the unavailability of accessible information makes it infeasible. However, since the first open simulation has been validated, the study deems it acceptable to extrapolate the results to the implementation of the heat pump, considering it a valid approach.

To describe how the study has implemented every part of the software, every step of the simulation is explained and relationated with the theory.

3.1 Fan implementation

As the machinery simulated has a very closed interval of possible mass airflows, the first step is choose the fan used in this cases. With the information in the Fig. 3, a mathematical approximation of the pressure/mass airflow curve has been done. With the mathematical approximation, and knowing the mass airflow provided by the chamber specifications, the pressure provided by the fan is obtained. Besides, the energy consumption is provided by the provider of the fan, which is 1.1 kW in normal conditions.

In this particular case, the Sodeca CAS-S 248-1.5 fan has been chosen as it is capable of efficiently operating within the mass airflow range of 250 kg/h to 350 kg/h, which aligns with the requirements of the process. This fan is suitable for achieving the desired depression of approximately 3 kPa while ensuring effective airflow management within the specified mass airflow interval. It is also the real one in the plant where the data come from.

Once the equation in the Fig. 9 is obtained, the code can be implemented.

$$P = -3 \cdot 10^{-6} \cdot \dot{m}_{air}{}^2 + 0.8 \cdot 10^{-3} \cdot \dot{m}_{air} + 3{,}9994 \qquad (17)$$

Where:

- P is the pressure produced by the Fan.

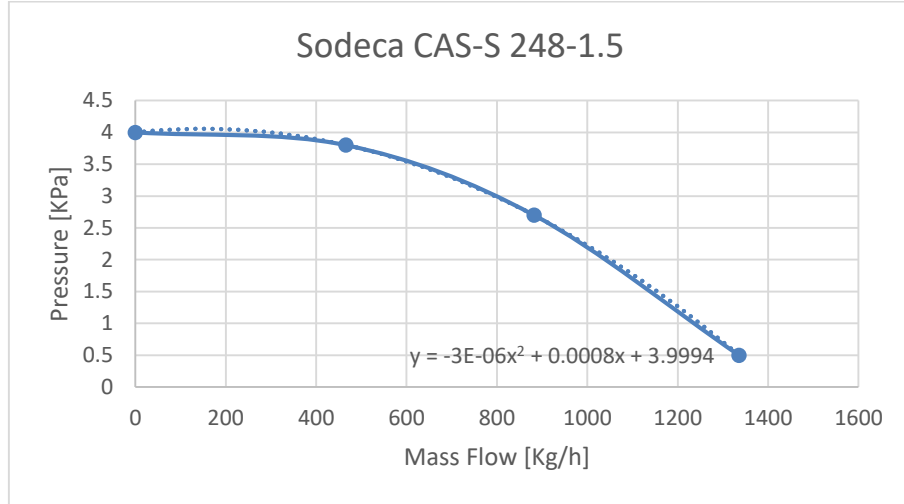- $\dot{m}_{air}$ is the airflow needed in the process.

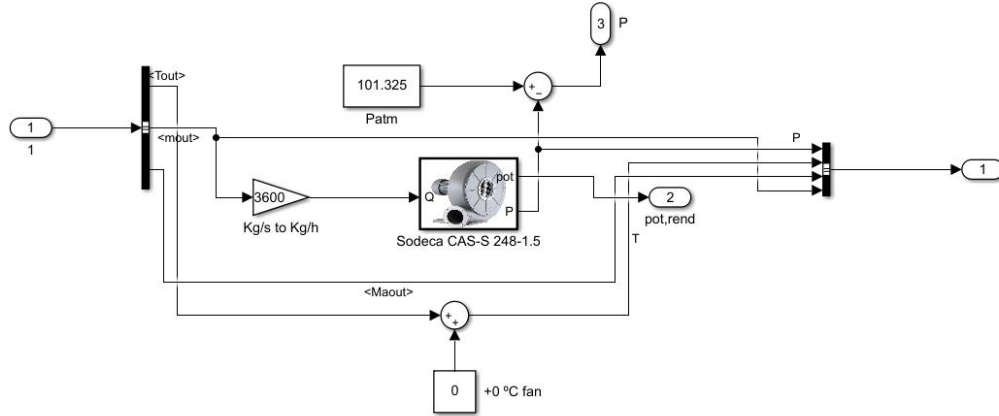*Figure 9: Pressure/Mass airflow diagram and the equation to approximate the behavior.*

Figure 10: Simulink coding and schema of the fan simulation.

3.2 Filter Implementation

As the mass airflow is known by the chamber simulation, the filter implementation is dedicated to know how many filter are needed and the drop pressure perceived. As the theory explain, in this simulation of a factory food process, the minimum filter needed is an HEPA filter. Following the provider recommendations, this type of filter need a pre-filter. The filters chosen for the simulation have the characteristics shown in the table 1.

Table 1: Characteristics of the filters implemented. [22]

Use	Filtering capacity	ΔP [kPa]	Airflow capacity [m3/h]
Pre Filter Coarse	G4 60%	0.055	3400
Filter	ePM1 85%	0.17	3400
HEPA Filter	E12	0.27	3400

As it can be seen, only one filter for each is enough for the interval of airflow the study is taken in count.
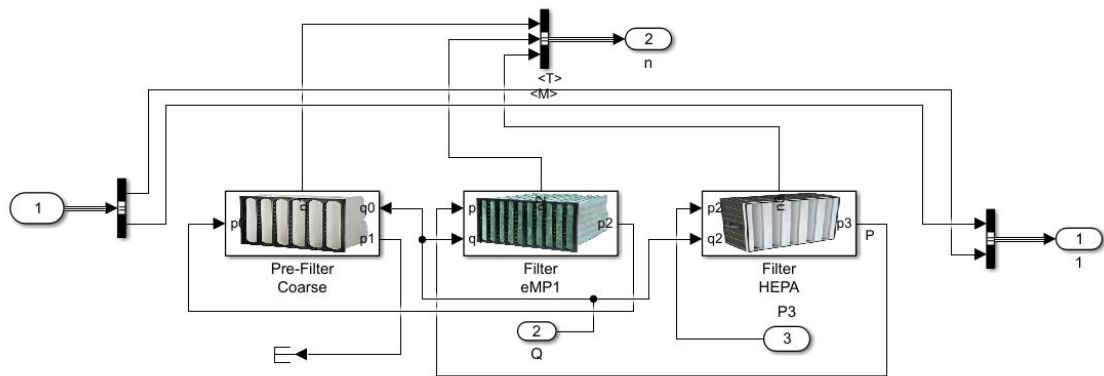

Figure 11: Simulink coding and schema of the filtering simulation.

3.3   Heater Implementation

Following the literature review, the temperature of the inlet airflow is determined by the powder requirements, the temperature from the environment is out of control and the mass airflow is determined by the chamber simulation. This means that the airflow requirements of the process is absolutely known. Because of that, the power required by the airflow process is also determined by the equation (4) and (13).

To obtain the use of mass flow of natural gas, the study considered that the heat transfer is done by a heat exchanger with a performance of 0.85 [11]. The heat transferred by the gas is obtained by the LCV (Low Calorific Value). The inlet temperature of the combustion chamber is considered equal to the environment temperature. The outlet temperature is considered the same temperature of the outlet process airflow plus 5°C, due the minimum temperature between the two airstreams is taken as 5°C. Finally, with the heat required from the process airstream, the diference of temperatures of the gases in the combustion chamber and the LCV of the natural gas, the gas needed is obtained. The AF value used is 0.98 following the literature [11].The LCV used is 47.3 MJ/kg [23]. The equation (18) is obtained and implemented.

$$\dot{q}_{req} + \dot{m}_{gas} \cdot \left(1 + \frac{9.52}{AF}\right) \cdot cp_a \cdot \Delta T_{cham} = \dot{m}_{gas} \cdot LCV_{gas} \quad (18)$$

Where:

- $\dot{q}_{req}$ is the heat required by the process

- $\dot{m}_{gas}$ is the mass flow of the natural gas.

- AF is the air fuel value.

- cp_a is the specific heat of the air.

- ΔT_{cham} is the difference of temperatures between the inlet and outlet combustion air.

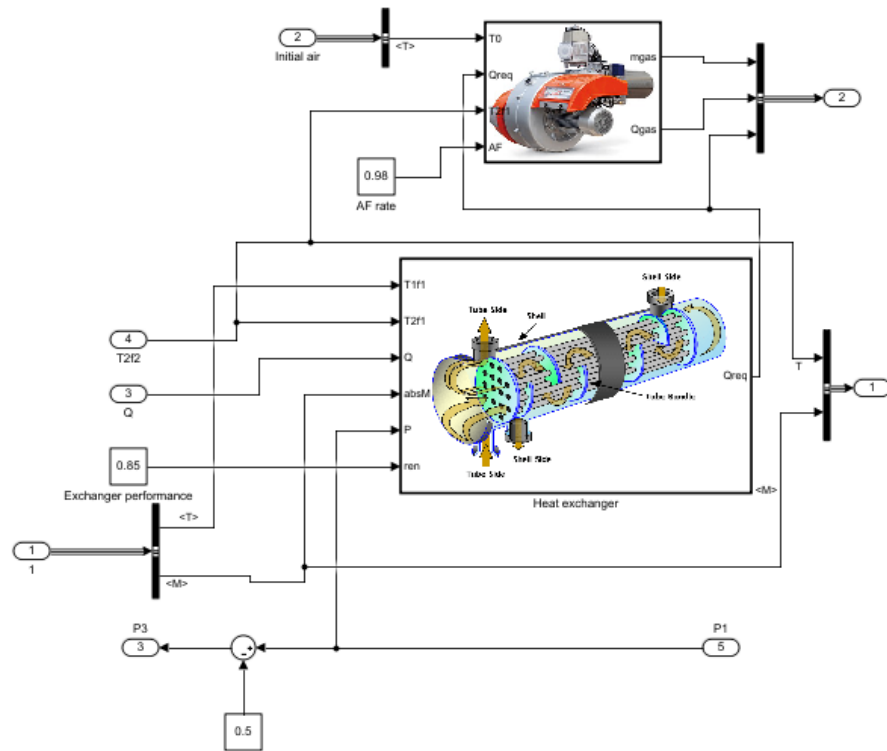- LCV_{gas} is the Low Combustion value of the natural gas.

Figure 12: Simulink coding and schema of the burner and the heat exchanger.

The mass flow of natural gas is used as an indicator of energy used in future analysis.

3.4   Chamber Implementation

The implementation the chamber begins by fixing the variables which are determined by the powder and the feed characteristics.

Table 2: Variables determined by the powder and the feed characteristics.

Type	Variable	Unit
Air characteristics	Inlet temperature	ºC
	Outlet temperature	ºC
	Inlet Moisture Content	kg water/kg air
Feed characteristics	Mass flow	kg/s
	Feed Temperature	ºC
	Solid content in the feed	kg Solid/kg water
	Specific heat of the solid	kJ $ºC^{-1}$ kg^{-1}
Powder characteristics	Moisture Content	kg water/kg Solid
	Powder Temperature	ºC

Using the pre-fixed variables of the table 2 and the equations (5), (8), (9), (10), (11), (12), (13) the variables of the table 3 are obtained.

Table 3: Variables obtained by the equations (5), (8), (9), (10), (11), (12), (13) and the variables of the table 2.

Type	Variable	Unit
Air characteristics	Inlet Mass airflow	kg/s
	Outlet Mass airflow	kg/s
	Outlet Moisture Content	kg water/kg air
Powder characteristics	Mass flow powder	kg/s
	Mass flow Solids of the powder	kg/s

The loses in the drying chamber are considered zero for simplification of the calculations.
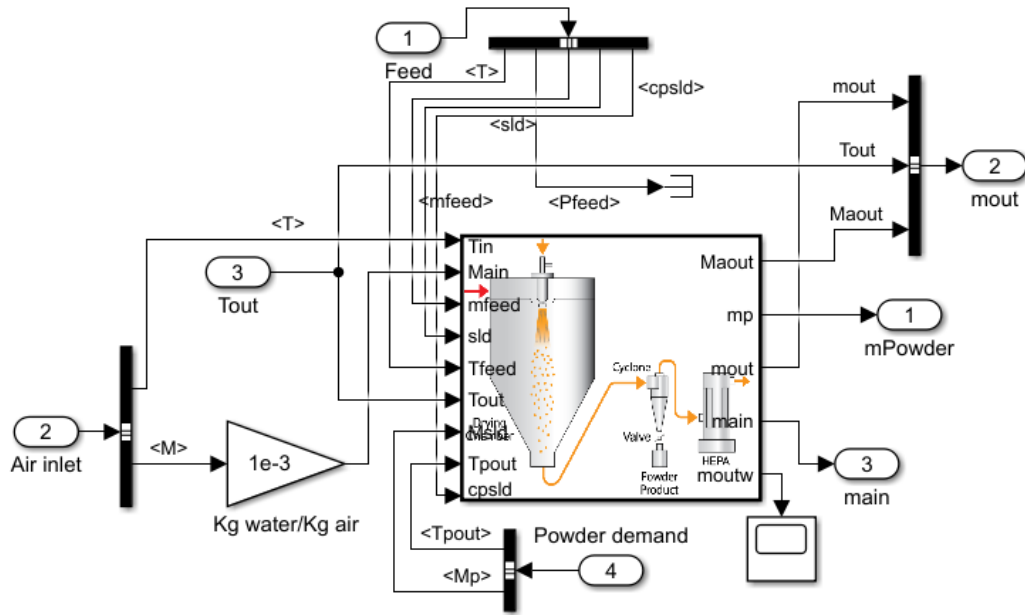
Figure 13: Simulink coding and schema of the drying chamber, the cyclone and filter.

After this process and because there is not a thermodynamically reason to do it, the separation of the air and the powder is considered perfect after the cyclone and the bag filter. That means that every solid part in the feed is obtained in powder form after the drying chamber. The drop of the pressure has taken in count when chosen the fan. The drop of the pressure taken in count has been 1kPa for the cyclone and the bag filter together.

3.5 Heat Pump Implementation

As the exhaust airflow is absolutely determined by the outlet air of the chamber, the energy available to recover is all the energy susceptible to be recollected by the evaporator of the heat pump.

Figure 14: Schema of the heat pump and the air streams.

The selected refrigerant for the system is R1233zd, which belongs to the fourth generation of refrigerants. This refrigerant of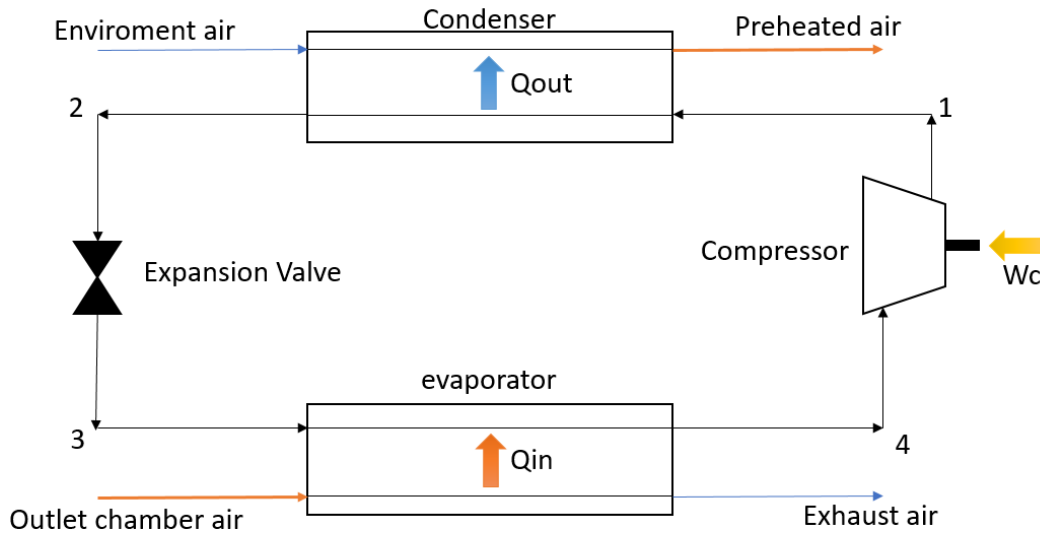fers the advantage of being able to condense at high temperatures while operating at relatively low pressures. By working at lower pressures, the need for specialized personnel trained to handle high-pressure conditions is mitigated.

The possibility of using a cascade heat pump, with a condenser operating at high temperatures and an evaporator operating at even lower temperatures, was considered. However, the decision was made to prioritize a simple recovery system. As a result, the condenser temperature was set at 100°C, while the evaporator temperature was maintained at 5°C. This configuration allows for efficient heat transfer and simplifies the overall system design and operation.

The outlet chamber air temperature is between 90ºC and 110ºC and the environmental air is between 0ºC and 20ºC. Besides, the objective is to preheat the air process so that means that the condenser has to be in a relative high temperature during the condensation. Both temperatures are considered different enough compared with the inlet temperature of air stream.

The conditions of design for the heat pump cycle are shown in the table 4. The cycle has been considered ideal. The Fig. 8 shows the cycle in the Pressure/Enthalpy curve.

Table 4: Design conditions of the heat pump.

Step	T [ºC]	P[bar]	h [kj/kg]	s [kJ $ºC^{-1}$ kg^{-1}]
1	107	10	477	1.79
2	100	10	327	1.4
3	5	0.6	327	1.46
4	20	0.6	420	1.79

Using the equations (14), (15) and (16), the following design has been obtained.

$$\dot{W}_c = \dot{m}_{ref} \cdot 57 \tag{19}$$

$$\dot{q}_{out} = \dot{m}_{ref} \cdot 150 \tag{20}$$

$$\dot{q}_{in} = \dot{m}_{ref} \cdot 93 \tag{21}$$

Where:

- $\dot{W}_c$ is the work done by the compressor.

- $\dot{q}_{out}$ is the heat transfer done in the condenser.

- $\dot{q}_{in}$ is the heat transfer done in the evaporator.

As the aim of the heat pump is to transfer the maximum heat as possible, the $\dot{q}_{out}$ is defined as the heat needed to warm the process air from the environment air up to 95°C. This temperature is the condenser temperature but applying the $\Delta T_{min} = 5°C$. The temperature of the air stream after the heat pump and to the environment is always warmer than 25°C which is the maximum temperature of the evaporator plus the $\Delta T_{min} = 5°C$. Besides, the relations (21) and (22) are considered.

$$\dot{q}_{out} = \dot{q}_{in \, process \, air} \tag{22}$$

$$\dot{q}_{in} = \dot{q}_{out \, exhaust \, air} \tag{23}$$

Where:

- $\dot{q}_{out}$ is the heat transfer done in the condenser.

- $\dot{q}_{in \, process \, air}$ is the heat transfer received by the process air.

- $\dot{q}_{in}$ is the heat transfer done in the evaporator.

- $\dot{q}_{out \, exhaust \, air}$ is the heat transfer delivery by the exhaust air.
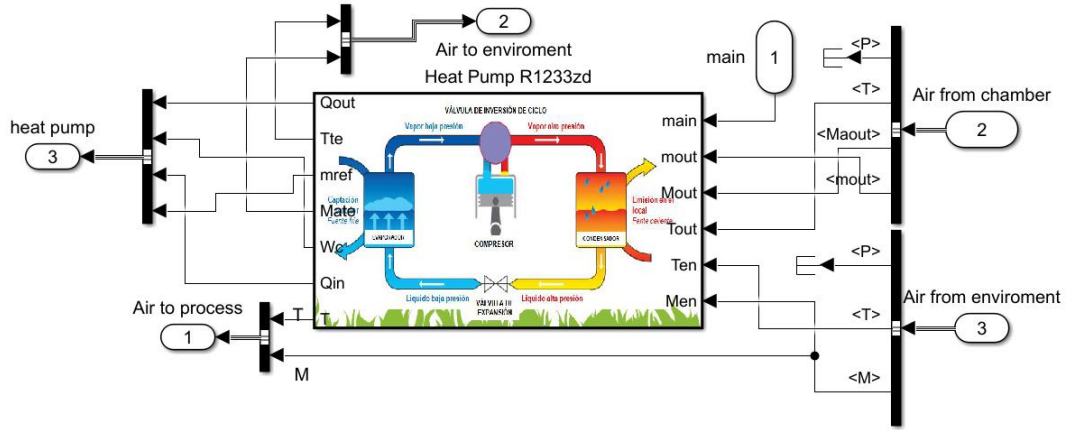
Figure 15: Simulink coding and schema of the heat pump.

Applying the design of the head pump and the equations (4), (13), (14), (21) and (22) the following variables are obtained.

Table 5: Variables obtained by the equations (4), (13), (14), (21), (22) and the design of the heat pump.

Type	Variable	Unit
Exhaust air	Temperature to environment	ºC
Process air	Temperature to process	ºC
Heat Pump	$\dot{W}_c$, $\dot{q}_{out}$, $\dot{q}_{in}$	kW
	Mass flow of refrigerant	kg/s

4 Results

In this part of the thesis the simulation designed is verified. After this first step, the model of the heat pump recovery is tested using the simulation verified.

At the end of this chapter and with the results obtained, the economic feasibility is studied.

4.1   Verification of the Simulation without heat recovery

Following the aims of the study, the results of the first simulation are contrasted with the data of a Production Minor in the table 6. In the table 7, the variables fixed by the available data are showed. The information is obtained from a test done in a Production Minor during a test after-readjusting the PID system. Because of that, the feed is a single sample containing an aromatic plant extract. Besides, the heat device implemented in the test is an electric heater. To be able to compare the information available, the $\dot{q}_{req}$ is compared. It is the energy required to warm the air from the environment air temperature to the inlet temperature of the chamber (T_{in}). As the theory explains, the direct heat transmit all the energy from the resistors to the air. Then, all the energy delivered by the electric heater is considered the heat received by the air. This allow the comparison of variables possible. The powder obtained has not been analyzed. Because of that, the study consider the absolute evaporation of the inlet water. This assumption is far from the reality because the regular moisture content in the powder obtained in this kind of machinery is more or less 4%. That means, in the worse case for the assumption, which is the one with more $\dot{m}_{feed}$, an absolute error of the $\dot{m}_{w\ evap}$ of 0.68 kg/s. After this explanation of how the study compare the information, the results are presented in the table 6 and discussed in the chapter 4.1.

Table 6: Verification of different variables of the Drying Chamber simulation.

T_{in}	T_{out}	$\dot{m}_{feed}$	$\dot{q}_{req}$	$\dot{q}_{req\ sim}$	Error	$\dot{m}_{w\ evap}$	$\dot{m}_{w\ evap\ sim}$	Error
[ºC]	[ºC]	[kg/s]	[kW]	[kW]	[%]	[kg/s]	[kg/s]	[%]
240	90	34	23	19	-17.4	17	16.6	-2.4
230	100	30	22	18	-18.2	15	14.5	-3.3
220	110	25	21	17	-19.0	12.5	12.5	0
210	110	22	20	15.5	-22.5	11	10.9	-0.9
200	100	23	19	15	-21.1	11.5	11.5	0.0
190	90	23.5	18	14.8	-17.7	11.8	11.6	-1.7

Table 7: Fixed data by the available data.

Variable		Unit
Temperature of the environment	20	ºC
Temperature of the feed	60	ºC
Solid content in the feed	50%	%
Powder temperature and Moisture	-	-

Figure 16: Production Minor made by GEA, NIRO S/A.

To contrast the gas consumption of the indirect heater, the data is compared in the table 8.

Table 8: Verification of different variables of the heater simulation.

T_{in}	T_{out}	$\dot{m}_p$	$\dot{m}_{gas}$	$\dot{m}_{gas\ sim}$	Error	$\dot{m}_{exhaust}$	$\dot{m}_{exhaust\ sim}$	Error
[ºC]	[ºC]	[kg/h]	[kg/h]	[kg/h]	[%]	[kg/s]	[kg/s]	[%]
40	250	30 000	149.24	151.2	+1.3	1517	1620	+6.8

Where:

- T_{in} is the inlet temperature in the combustion chamber.

- T_{out} is the outlet temperature in the combustion chamber.

- $\dot{m}_p$ is the mass flow of process air.

- $\dot{m}_{gas}$ is the mass flow of burned gas.

- $\dot{m}_{exhaust}$ is the mass flow of the exhaust gas.

- $\dot{m}_{gas\ sim}$ is the mass flow of burned gas in the simulation.

- $\dot{m}_{exhaust\ sim}$ is the mass flow of the exhaust gas in the simulation.

The data available is only one sample of a big indirect heater. The data has been collected during a regular visit. In the discussion chapter, the validity of this verification is discussed.

4.2   Results of the heat pump recovery

To obtain the results of the heat pump, different variables from the simulation with the heat pump and the simulation without the heat pump have been compared. The table 9 shows the results. The T_{te} is considered equal to T_{out} in the simulation without heat pump.

Table 9: Comparison of different variables of the simulation with and without heat pump.

T_{in}	T_{out}	$\dot{m}_{feed}$	$T_{te\ HP}$	$\dot{m}_{gas}$	$\dot{m}_{gas\ HP}$	$\dot{W}_{c\ HP}$
[ºC]	[ºC]	[kg/s]	[ºC]	[kg/h]	[kg/h]	[kW]
240	90	34	46	1.31	0.89	2.0
230	100	30	55	1.28	0.85	2.1
220	110	25	64	1.22	0.80	2.1
210	110	22	64	1.11	0.70	2.0
200	100	23	54	1.10	0.67	2.1
190	90	23.5	44	1.10	0.63	2.1

Where:

- T_{in} is the drying chamber inlet temperature airflow.

- T_{out} is the drying chamber outlet temperature airflow.

- $\dot{m}_{feed}$ is the mass flow of the feed in the drying chamber.

- $\dot{m}_{gas}$ is the mass flow of natural gas in the heater.

- $\dot{m}_{gas\ HP}$ is the mass flow of natural gas in the heater in the simulation using a heat pump.

- $T_{te\ HP}$ is the exhaust temperature in the simulation using a heat pump.

- $\dot{W}_{c\ HP}$ is the compressor work in the simulation using a heat pump.

The variables used are the same variables as the table 7. The different combinations of variables are the same as the real data available to be coherent.

4.3 Economic feasibility

Following the aims of this study, the economic feasibility of this new technology implementation is determined. To do it, the price of the installation and the save of money due it is taken in count. The heat pump needed has a heat output power of 5.5kW and a compressor power of 2.1kW.

Nowadays, the price of the natural gas is very volatile in Europe but the average price before these irregular times was 0.028€/1kWh. The average saving of natural gas is 0.43kg/h as can be seen in the table 10. This means a 5.6 kW of gas savings using the LCV.

Because the price of the natural gas is very volatile in Europe, the energy price in Europe is also very volatile. The average price in stable times was 0.13€/kWh.

The monetary saving related with the gas savings is 0.16 €/h.

The monetary spending related with the compressor power is 0.26 €/h.

This means that the investment done in the heat pump will never be amortized in this scale because the electricity price related to the compressor is higher than the monetary saving in the natural gas. The average monetary loses using the heat pump is 0.1 €/h.

The reason to swift from a pure gas consumption to a hybrid gas-electric consumption is not always the price as is discussed in the chapter 4.2.

5 Discussion

5.1 Verification of the Simulation without heat recovery

About the difference between the energy requirements in the simulation and the data, as it can be seen in the table 6, the simulation is having wrong values of the energy requirements of the inlet mass airflow. The average of the error is $+19.3\%$. This error could be as a result of the energy loses which are neglected in the model. As it is almost a constant error, it can be readjusted by increasing the energy requirements by 19.3%. With this change done, the simulation is giving results between -3.3% and $+1.8\%$ of accuracy of the energy requirements of the inlet mass airflow.

The accuracy of the simulation results in the evaporating capacity is quite high, the interval of accuracy is $-3,3\%$ and 0%. As it has been explained in the results chapter, this result is expected to be lower than the reality because part of the water is in the final powder.

The accuracy of the simulation results in the gas consumption is also quite high with an error of $+1.3\%$. The data is obtained from a machinery much bigger than the needed by the target model of this study. Nevertheless, the simulation of the heat exchanger is not taking in count this size premise in any point. Because of that, the heat exchanger simulation is verified in an interval of use higher than the desired but the study considered this results extrapolable and satisfactory.

5.2   Heat pump recovery

Following the line of working in the verified zone, the results are compared in the same combination of variables for maintain the coherence. The results of the difference of gas consumption are in the table 10.

Table 10: Comparison of gas consumptions

T_{in}	T_{out}	$\dot{m}_{feed}$	$\dot{m}_{gas}$	$\dot{m}_{gas\,HP}$	$\Delta\dot{m}_{gas}$
[ºC]	[ºC]	[kg/s]	[kg/h]	[kg/h]	[kg/h]
240	90	34	1.31	0.89	-0.42
230	100	30	1.28	0.85	-0.43
220	110	25	1.22	0.80	-0.42
210	110	22	1.11	0.70	-0.41
200	100	23	1.10	0.67	-0.43
190	90	23.5	1.10	0.63	-0.47

The reduction of gas consumption per hour is clear and it has an average of 0.43kg/h. This reductions comes with the consumption of the compressor, which the average is 2.07 kW. To be able to compare, the gas consumption represents a reduction of 5.6 kw of power. Therefore, the power saving is an average of 3.53kW. Althoug this result is clear, the difference of quality of the resource between the electricity and the gas is clear, been the electricity much valuable. Nevertheless this issues, one of the key objectives of this study was to achieve a reduction in natural gas consumption. In this regard, the results obtained have been deemed satisfactory. By implementing the proposed system and optimizing various parameters, the study has successfully demonstrated the potential for reducing the reliance on natural gas in the drying process. This achievement aligns with the overall goals of energy efficiency and sustainability in industrial operations.

6 Conclusions

As the results has shown in the tables 6, 8 and 9, the numbers obtained are accurate enough in comparison with the real data available. The error expected in the simulation is less than 5% in every variable expect for the exhaust air from the heat exchanger, which is 6.8%, which is satisfactory enough.

The drying results obtained from the drying chamber model were verified using a medium-sized machinery, namely Production Minor Spray Dryer manufactured by GEA, NIRO S/A.

The implementation of a heat pump in the system leads to an average reduction in natural gas consumption of 0.43 kg/h. However, it is important to note that this gas savings is accompanied by an additional electricity consumption of 2.1 kW by the compressor of the heat pump.

The savings in natural gas are not high enough to economically compensate the new use of electricity involve in the heat pump. The average monetary loses is 624€/year by producing 6240h/year.

Nevertheless, the installation of a heat pump energy recovering in this size spray drying machinery reduces dependency of natural gas by a 36%.

In future studies, it is recommended to verify the simulation model with other models of spray drying machinery to enhance the robustness and generalizability of the findings. By testing the model against different types and sizes of spray dryers, a more comprehensive understanding of the system's behavior can be obtained. Additionally, gathering and incorporating a larger dataset with varied operating conditions and product characteristics will further strengthen the validity and accuracy of the simulation model. This expanded verification process will contribute to a more comprehensive and reliable analysis of the spray drying process.

6.1 Perspectives

In regard to sustainability, the heat recovery system results in a decrease in power consumption by 3.53 KW and a 36% decrease in natural gas usage. This is highly commendable as it reduces dependency on fossil fuels and enhances efficiency.

References

[1] T. Kudra, "*Energy Aspects in Drying,*" Drying Technology, vol. 22, pp. 917-932, 2004. DOI: 10.1081/DRT-120038572.

[2] S.N. Moejes et al., "*Closed-loop spray drying solutions for energy efficient powder production,*" Innovative Food Science and Emerging Technologies, vol. 47, pp. 24-37, 2018. ISSN: 1466-8564. DOI: 10.1016/j.ifset.2018.01.005.

[3] Arun S. Mujumdar, "*Research and Development in Drying: Recent Trends and Future Prospects,*" Drying Technology, vol. 22, no. 1-2, pp. 1-26, 2004. DOI: 10.1081/DRT-120028201.

[4] Uçal, E.; Yildizhan, H.; Ameen, A.; Erbay, Z. et al., "*Assessment of Whole Milk Powder Production by a Cumulative Exergy Consumption Approach,*" Sustainability, vol. 15, no. 15, article 3475, 2023. DOI: 10.3390/su15043475.

[5] M. Camci, "*Thermodynamic analysis of a novel integration of a spray dryer and solar collectors: A case study of a milk powder drying system,*" Drying Technology, vol. 38, no. 3, pp. 350-360, 2020. DOI: 10.1080/07373937.2019.1570935.

[6] S.K. Patel and M.H. Bade, "*Energy analysis and heat recovery opportunities in spray dryers applied for effluent management,*" Energy Conversion and Management, vol. 186, pp. 597-609, 2019. ISSN: 0196-8904. DOI: 10.1016/j.enconman.2019.02.065.

[7] P. Schuck, A. Dolivet, and Méjean, "*Relative humidity of outlet air: the key parameter to optimize moisture content and water activity of dairy powders,*" Dairy Sci. Technol., vol. 88, pp. 45-52, 2008. DOI: 10.1051/dst:2007007.

[8] A.A. Dolinsky, "*HIGH-TEMPERATURE SPRAY DRYING,*" Drying Technology, vol. 19, no. 5, pp. 785-806, 2001. DOI: 10.1081/DRT-100103770.

[9] K. Masters, "*FULL CONTAINMENT SPRAY DRYING,*" Drying Technology, vol. 17, no. 10, pp. 2341-2348, 1999. DOI: 10.1080/07373939908917687.

[10] C.G.J. Baker and K.A. McKenzie, "*Energy Consumption of Industrial Spray Dryers,*" Drying Technology, vol. 23, no. 1-2, pp. 365-386, 2005. DOI: 10.1081/DRT-200047665.

[11] C.R. da Silva et al., "*Thermodynamic characterization of single-stage spray dryers: Mass and energy balances for milk drying,*" Drying Technology, vol. 35, no. 15, pp. 1791-1798, 2017. DOI: 10.1080/07373937.2016.1275675.

[12] V. Westergaard, "*Milk powder technology,*" Evaporation and Spray-Drying, GEA Niro A/S, Copenhagen, 2001.

[13] M. Winkler, "*Spray Drying - Freund Vector*," Freund-Vector. [Online]. Available: https://www.freund-vector.com/technology/spray-drying/.

[14] SODECA, "*Manufacturer of industrial fans and extractors*," SODECA. [Online]. Available: https://www.sodeca.com/es. Accessed: Month day, year.

[15] EPA, HEPA & ULPA filters | Camfil, Camfil. [Online]. Available: https://www.camfil.com/en/products/epa-hepa-and-ulpa-filters.

[16] "*HTV-N Indirect Process Air Heater - Babcock Wanson*," Babcock Wanson, 2021. [Online]. Available: https://www.babcock-wanson.com/products/industrial-process-air-heaters/htv-n-indirect-process-air-heater/.

[17] Spray Drying Nozzles, "*Feedstock - Spray Drying Nozzles*," Spray Drying Nozzles. [Online]. Available: https://spraydryingnozzles.com/feedstock/.

[18] GEA, "*Spray Dryers | GEA Dryers & Particle Processing Plants*," GEA engineering for a better world. [Online]. Available: https://www.gea.com/en/products/dryers-particle-processing/spray-dryers/index.jsp.

[19] CycloTwist, "*Ciclones Industriales, MXCYW-001-028*," Everything in Ventilation SA CV. [Online]. Available: https://ventdepot.mx/products/cyclotwist-ciclones-industriales-mxcyw-001-028?variant=40573255516245.

[20] U.S. Air Filtration, Inc., "*Top 3 Reasons Filter Bags Fail*," U.S. Air Filtration, Inc. [Online]. Available: https://www.usairfiltration.com/top-3-reasons-filter-bags-fail/.

[21] Danfoss, "*We engineer tomorrow to build a better future*," Danfoss. [Online]. Available: https://www.danfoss.com/en/.

[22] Camfil, "*Panel filters | Camfil*," Camfil. [Online]. Available: https://www.camfil.com/en/products/general-ventilation-filters/panel-filters.

[23] P. Martina et al., "*Diseño y construcción de un calorímetro de junkers para determinación del poder calorífico del biogás*," Avances en Energías Renovables y Medio Ambiente, vol. 15, pp. 1-9, 2011. ISSN: 0329-5184. [Online]. Available: https://core.ac.uk/download/pdf/328878202.pdf.

Appendix A

The code used in the simulations is in the next pages:

Filters

```
function [p1,n1]= fcn(q0,p0)


  n1=q0/3400;
  n1=ceil(n1);

  p1=p0+0.055;

  end
```

Heater

```
function Qreq  =fcn(T1f1,T2f1,Q,absM,P,ren)


    y =(1-absM*10^(-3));
    z = absM*10^(-3);



    P1= P*0.01;
    Q1= Q;

    h2f1 = XSteam('h_pt',P1,T2f1);
    h1f1 = XSteam('h_pt',P1,T1f1);



    Qreq1 = (Q1*y)*(1.005*(T2f1-T1f1))  + (Q1*z)*(h2f1-h1f1);


    Qreq= Qreq1/ren;

end
```

```matlab
function [mgas,Qgas]= fcn(T0,Qreq,T2f1,AF)

T2f2=T2f1+5;



mgas=Qreq/(47.1e3-((1+(9.52/AF)))*(T2f2-T0)*1.005);
Qgas=mgas*47.1e3;




end
```

Chamber

```matlab
function [Maout,mp,mout,main,moutw]= fcn(Tin,Main,mfeed,sld,Tfeed,Tout,Msld,Tpout,cpsld)

    cpa=1.005;
    cpv=1.67;
    cpw=4.2;
    dhvap=2500;

    mfeedsld=mfeed*sld;
    mfeedw=mfeed*(1-sld);

    mpsld=mfeedsld;
    mpw=mpsld*(Msld/(1-Msld));

    hp = mpsld*Tpout*cpsld + mpw*Tpout*cpw;
    hfeed= mfeedsld*cpsld*Tfeed + mfeedw*cpw*Tfeed;

    Maout= (((cpa*Tin)+(Main*(cpv*Tin+dhvap))-(cpa*Tout))*(mfeedw-mpw)-(Main*(hp-hfeed)))/((hp-hfeed)+((cpv*Tout)+dhvap)*(mfeedw-mpw));

    main=(mfeedw-mpw)/(Maout-Main);
    moutw= mfeedw+Main*main-mpw;
    mout=moutw+main;
    mainw=main*Main;
    mp=mpw+mpsld;
```

Fan
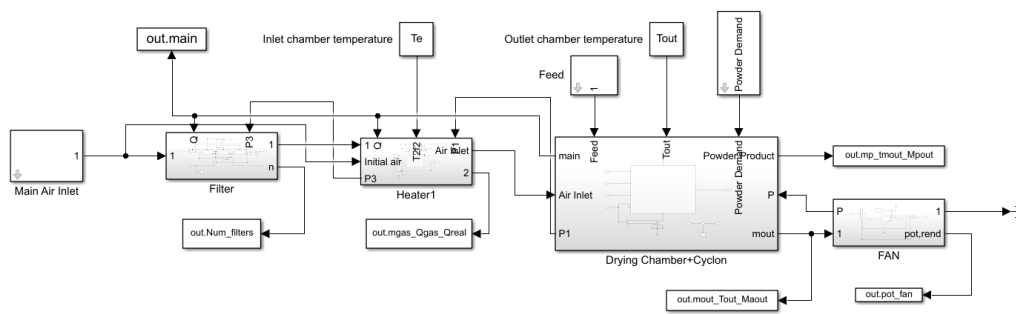
```matlab
function [pot,P]= fcn(Q)

P=0;

|

pot= 1.1;


P =-3e-06*Q^2 + 0.0008*Q + 3.994;


end
```

A4

General view without heat pump

Heat Pump:

```
function [Qout,Tte,mref,Mate,Wc,Qin,T]= fcn(main,mout,Mout,Tout,Ten,Men)
cpa= 1.005;
cpv= 1.67;
Men=Men/1000;
T=95;
Qin=main*Men*cpv*(100-Ten)+main*(1-Men)*cpa*(100-Ten);
mref=Qin/150;
Wc=mref*57;
Qout=Qin-Wc;
Tte = Tout-(Qout/(mout*Mout*cpv+mout*(1-Mout)*cpa));
Mate=Mout;

end
```

General view with heat pump